

Dynamics of the Intermolecular Transfer Integral in Crystalline Organic Semiconductors

Alessandro Troisi*[†] and Giorgio Orlandi[‡]

Department of Chemistry, University of Warwick, Coventry, CV4 7AL, U.K., and Dipartimento di Chimica 'G. Ciamician', Università di Bologna, via F. Selmi 2, 40126 Bologna, Italy

Received: September 24, 2005; In Final Form: January 5, 2006

In organic crystalline semiconductor molecular components are held together by very weak interactions and the transfer integrals between neighboring molecular orbitals are extremely sensitive to small nuclear displacements. We used a mixed quantum chemical and molecular dynamic methodology to assess the effect of nuclear dynamics on the modulation of the transfer integrals between close molecules. We have found that the fluctuations of the transfer integrals are of the same order of magnitude of their average value for pentacene and anthracene. Under these conditions the usual perturbative treatment of the electron–phonon coupling is invalid, the band description of the crystal breaks down and the charge carriers become localized. Organic crystals of pentacene and anthracene, even in the absence of defects, can be regarded as disordered media with respect to their charge transport properties. These results suggest that the dynamic electronic disorder can be the factor limiting the charge mobility in crystalline organic semiconductors.

1. Introduction

The theoretical understanding of the charge transport mechanism in ordered organic semiconductors is still unsatisfying. Notwithstanding decades of investigation,^{1–3} several contradictions between known conduction models and experimental evidence suggest that the framework developed for the study on inorganic semiconductors is somewhat inadequate for the rationalization of the transport properties of organic materials.⁴ For example, in a pure thin film of pentacene, the hole mobility μ decreases with the temperature up to room-temperature according to a power law ($\mu \sim T^{-n}$),⁵ a phenomenology compatible with the band transport mechanism. However, the fitting of the experimental data with the phenomenological models indicates a mean free path of the hole comparable with the crystal unit cell,^{6,7} a fact in contradiction with the delocalized picture that is implied by the band model.

It is convenient to recall the structural and electronic differences between inorganic and organic semiconductors to identify the origin of the different transport mechanisms. Organic semiconductors are narrow band materials; i.e., the electronic interaction between the molecules in the crystal is much weaker than the interaction among atoms in silicon or germanium. On the other hand, the unit cell in organic materials is much larger, causing an effective mass for the charge carrier comparable to that of wide band materials.⁸ The weak attractive interaction between the constituent of an organic crystal makes these materials very soft and the consequences for their transport properties can be dramatic. This aspect is very well exemplified by several studies in the related study field of charge transfer in donor–bridge–acceptor systems. If the “bridge” is made by covalently bonded atoms (as in silicon) the coupling between donor and acceptor can be considered constant (Condon approximation).⁹ When the transfer takes place through non-bonded molecules (as in an organic crystal), thermal motions

cause a fluctuation of the donor–acceptor coupling that affects the charge transfer rate.¹⁰ Examples of noncovalently bonded bridges that produce a strong fluctuation of the intermolecular coupling include, among others, the DNA base pair,¹¹ some proteins,¹² or the solvent¹³ in specially designed systems. The experience from charge transfer studies suggests that also the electronic coupling between (noncovalently bonded) molecules in an organic semiconductor can be strongly influenced by the thermal motions.

In this paper we assess the importance thermal motions in the modulation of the intermolecular coupling relevant for the charge transport in organic semiconductors. We present the results for the pentacene, probably the most studied compound for organic electronics forming ordered crystal or thin film structures. Results relative to the anthracene will be also presented for comparison. In the next section we describe the semiclassical approach used to perform this study. In the third section we present the results and some justification a posteriori of the adopted computational model. Our findings will be summarized in the last section where we relate our approach to the others presented in the recent literature.

2. Method

Model. The full quantum description of the electron–phonon coupling in an organic semiconductor is complicated and it usually requires some assumption on the coupling strengths that allows some sort of perturbative treatment.^{14,15} In this paper we adopt a semiclassical approach assuming that the nuclear motions of the crystal can be treated classically whereas the charge carriers are treated quantum mechanically, an assumption often taken in the study of conductive polymers. We use the following time-dependent one-particle (hole or electron) Hamiltonian:

$$H = \sum_i \epsilon_i a_i^\dagger a_i + \sum_{i \neq j} V_{ij}(t) a_i^\dagger a_j \quad (1)$$

where the operators a_i^\dagger and a_i create and annihilate a fermion

* Corresponding author. Phone: +44 024 7652 3228. Fax: +44 024 7652 4112. E-mail: a.troisi@warwick.ac.uk.

[†] University of Warwick.

[‡] Università di Bologna.

in a molecular orbital (MO) localized on the molecule i th. We assume one relevant MO per molecule (single band approximation), for example, the HOMO orbital if we are interested in the hole transport. The single band approximation may be insufficient in some circumstances,^{16,17} but the results of this paper can be easily extended to the general case. The time dependence of $V_{ij}(t)$ is imposed by the classical nuclear motions that (in this model) have the only effect of modulating the transfer integral. The approximations implied in this approach and some justifications are summarized below:

(i) A single band can be used to describe the electron/hole. Band calculations show that the bands originating from the HOMO and the LUMO do not mix with bands originating with other orbitals in most organic semiconductors including pentacene and that, therefore, a single band provides a valid description of the electron or hole mobility.

(ii) The phonons that couple with the electrons are low-frequency modes that can be treated classically. This point can and will be verified a posteriori. The semiclassical approach has the advantages that the effect of hundreds of optical phonon modes that are needed to describe the nuclear motions of an organic crystal is summed up in a unique time dependent quantity $V_{ij}(t)$.

(iii) The classical motion of the nuclei is marginally affected by the charge carrier wave function and $V_{ij}(t)$ can be seen as an external modulation. An extra positive (or negative) charge on a large molecule like pentacene causes minor changes in its molecular vibrational modes¹⁸ suggesting that the modulation of the transfer integral V_{ij} is not affected by the charge carrier distribution. The principal finding of this paper is not affected by this approximation that can be relaxed at a later stage.

(iv) We are neglecting the diagonal or Holstein coupling, i.e., the coupling of the matrix elements ϵ_i with the nuclear coordinates. These terms account for the deformation of the molecule when a net charge is on site i . The effect of Holstein coupling is extensively discussed in the literature and textbooks.¹⁹ Its main effect, in the small coupling regime appropriate to pentacene, is to produce band narrowing¹⁴ with consequent reduction of the charge mobility (whereas in the large coupling regime it is responsible of the formation of small polarons). This approximation is introduced only for simplicity because we will focus in this paper on the importance of off-diagonal electron–phonon coupling.

The main system investigated in this paper is a plane of crystalline pentacene, one of the reference standards for organic electronics. An ordered pentacene thin film can be grown on a SiO₂ substrate^{20–23} with the ab plane parallel to the substrate. Hole conduction takes place mostly within this plane (probably the first layer)²⁴ in a thin film transistor experimental setup. It was shown that the highest occupied band of the perfectly ordered (001) plane of pentacene can be expressed analytically as a function of three transfer integrals between the (unperturbed) HOMOs of the isolated molecule.²⁵ We investigate here the effect of thermal motions on these three transfer integrals.

Computational Details. We replicated the crystal unit cell²⁶ building a $3 \times 2 \times 2$ supercell (containing two layers of pentacene molecules in the ab plane). The dynamics of the system was studied with periodic boundary conditions employing the MM3 force field.²⁷ This force field is particularly suited to study conjugated organic molecules because it is coupled to a semiempirical evaluation of the bond order among sp² carbons that allows a correct description of the bond alternation. In this study we computed the bond order for an isolated single pentacene molecule and we run the simulation using the same

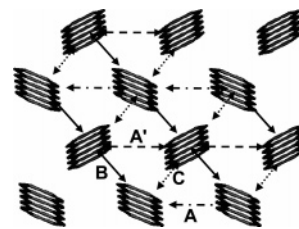


Figure 1. Six unit cells in the ab plane of pentacene (a portion of the supercell considered for the MD simulation). The arrows indicate the intermolecular couplings monitored along the MD, divided in four groups A (dashed–dotted), A' (dashed), B (solid) and C (dotted).

constant bond order for all the 24 pentacene molecules of the system. We run MD simulations at constant temperatures of 100, 200, and 300 K, using the Berendsen's algorithm²⁸ to simulate the presence of a thermal bath. The volume (and crystal cell parameters) was kept fixed to the value of ref 24 at all temperatures. The integration time step was set to 2 fs (the hydrogen atoms were kept at their equilibrium distance²⁹). The computer code Tinker^{30,31} was used to perform the classical MD simulation.

The electronic coupling between HOMO orbitals of two neighboring molecules was computed from the equation

$$V_{ij} = \langle \phi_i^0 | \hat{F}^0 | \phi_j^0 \rangle \quad (2)$$

where ϕ_i^0 and ϕ_j^0 are the unperturbed HOMOs of the two distinct molecules and \hat{F}^0 is the Fock operator of the system of the two bases built using the unperturbed density matrix (we used a similar approach in ref 11 and 13). Other researchers in the field of organic electronics often adopt the “dimer” method³² where the energy splitting of the HOMO orbitals in the molecular orbital calculation of two *identical* molecules is identified with $2|V_{ij}|$. In our case the two considered molecules are not identical at a given time because of the nuclear dynamics that we are explicitly taking into account. Therefore, we compute directly the matrix element V_{ij} using eq 2, valid also if the two considered molecules are nonequivalent.

We evaluated the transfer integral between HOMO orbitals every 30 fs with the INDO/S Hamiltonian, which proved to give results in reasonable agreement with more accurate DFT calculation.³² As reported in Figure 1, the close molecular pairs can be of type A, A', B and C. For each considered snapshot we computed 3 transfer integrals between couples of type A and A', and 6 transfer integrals between couples of type B and C. The 18 evaluations of the intermolecular coupling were the slowest part of the procedure that limited the length of the analyzed dynamics to 100 ps. We note that, in the crystal plane of interest, no molecule interacts with its image. Additional technical details on the coupling between MD and quantum chemical calculations are given in ref 13.

The very same procedure was applied to the ab plane of the crystalline anthracene,³³ displaying a packing similar to that of pentacene. This additional computation was done to verify that the characteristics shown in this paper focused on pentacene are likely to be general features of polyacenes and, probably, of all ordered, noncovalently bonded, organic semiconductors.

3. Results

A sample of the time variation of the three transfer integrals of type A, B, and C is given in Figure 2. We will begin the analysis by describing the distribution of the HOMO–HOMO coupling between molecular pair and neglecting its time dependence. Because the couplings A and A' behave similarly,

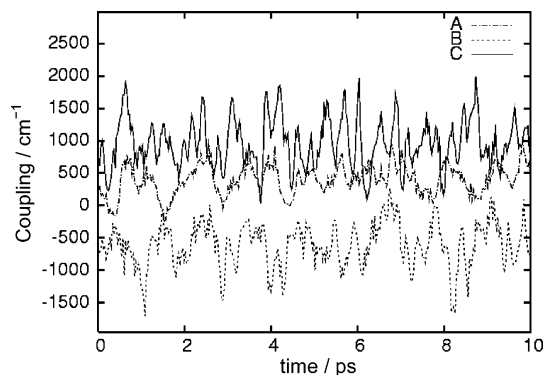


Figure 2. Time modulation of the transfer integrals due to thermal motions (300 K) for three molecular pairs of type A, B, and C (see Figure 1).

TABLE 1: Average Coupling and Variance of the Intermolecular Transfer Integral between Molecular HOMOs in Pentacene (Space Group $P1$) and Anthracene (Space Group $P2_1/a$) at Different Temperatures

	$T = 100$ K		$T = 200$ K		$T = 300$ K	
	$\langle V \rangle$	σ_V	$\langle V \rangle$	σ_V	$\langle V \rangle$	σ_V
Pentacene						
A	459.8	150.3	460.9	199.8	455.3	258.8
A'	477.2	150.5	485.5	207.1	476.6	262.1
B	-630.9	208.0	-626.0	291.3	-615.9	356.4
C	1018.4	237.5	1008.0	327.1	983.3	404.4
Anthracene						
A	-621.9	203.7	-616.7	275.8	-629.6	375.7
B	445.7	276.3	439.8	395.1	426.7	496.6

^a The higher symmetry of the anthracene crystal makes equivalent the transfer integrals A–A' and B–C.

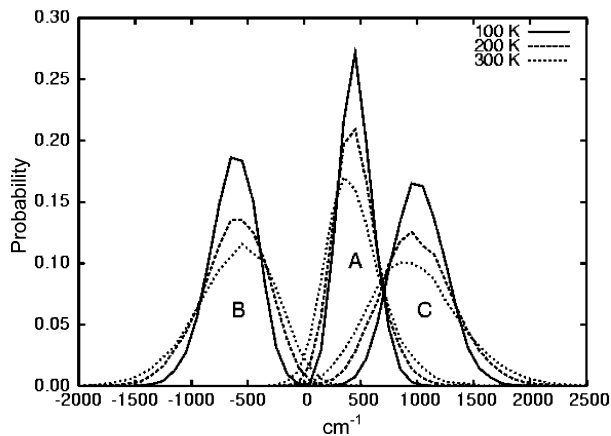


Figure 3. Distribution of the transfer integrals in solid pentacene at different temperatures.

we will mention only the former in the discussion. Table 1 shows the average couplings and the variance computed for the pentacene and the anthracene at different temperature. Couplings of the same type between different molecules are treated cumulatively in the calculation of the averages. Figure 3 displays the distribution of the A, B and C coupling for the pentacene at different temperatures. The distributions are Gaussian with width varying between 250 and 400 cm^{-1} at room temperature.³⁴ We have not performed calculations at a temperature lower than 100 K because, in the limit of low temperature, the classical approximation adopted for the crystal nuclei motions breaks down.

The variance of the transfer integrals coupling is extremely large and the modulation introduced by the nuclei is of the same

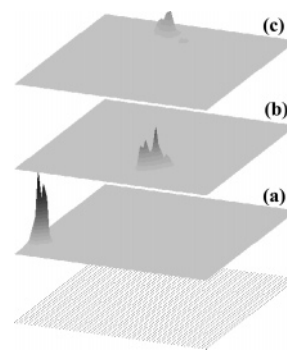


Figure 4. Localization of eigenstates due to thermal disorder (at 300 K). The charge densities, $\rho(x,y) = |\psi_i(x,y)|^2$, are reported for the ground state ($E = E_0$) (a) and states at energy $E - E_0 = 305 \text{ cm}^{-1}$ (b) and $E - E_0 = 500 \text{ cm}^{-1}$ (c). The dots in the lowermost part of the pictures indicate the position of the 3200 molecules in the supercell used to study the charge localization.

order of magnitude of the average coupling. To search for possible correlations between the intermolecular coupling V_K and V_L , we computed the statistical correlation between them, defined as

$$\text{cor}(V_K, V_L) = \frac{\langle V_K V_L \rangle - \langle V_K \rangle \langle V_L \rangle}{\sigma_{V_K} \sigma_{V_L}} \quad (3)$$

σ_{V_K} and σ_{V_L} being the standard deviation of the individual coupling. The correlation (computed between all the couples shown in Figure 1 at 300 K) is small ($0.1 < |\text{cor}(V_K, V_L)| < 0.25$) for pairs of intermolecular couplings that share a common molecule and negligible ($|\text{cor}(V_K, V_L)| < 0.1$) for independent couples of molecules. This observation can be very helpful for the modeling of the process because, to a very good degree of approximation, the intermolecular coupling fluctuation can be considered uncorrelated. The lack of correlation is due to the relatively large number of phonon modes that are coupled to the intermolecular transfer integral. Many low-frequency optical phonons are essentially dispersionless; i.e., they can be also treated as vibration localized on each molecule (as in the Einstein model). These modes contribute with independent phases to the time dependence of V_{ij} , and the overall coupling pattern is essentially random.

The effect of uncorrelated modulation is equivalent to the effect of *disorder* in the electronic structure, and its main effect is the *localization* of the hole wave function.^{35–37} The localization of the eigenfunctions (in the frozen conformation at a give time) of a system characterized by the parameters given in Table 1 can be easily evaluated. We built a large supercell containing 3200 pentacene molecules, coupled according to the pattern outlined in Figure 1, and we attributed random values to the transfer integrals following a Gaussian distribution with the parameters of Table 1 (i.e., derived from the computations on a small supercell). Figure 4 depicts the typical density distribution of the hole for several eigenfunctions of such a disordered system at 300 K. All eigenfunctions are localized within a few unit cells, and the ones represented in Figure 4 are just three samples taken at different energies (eigenvalues) to help their visualization. It should be remarked that each region of the plane has some eigenfunctions localized close to it and that eigenfunctions with close energy need not be localized in close regions of the plane. Localized wave functions have normally several nodal planes³⁶ and, for this reason, the charge density displays several peaks and valleys.

A quantitative measure of the degree of localization of an eigenfunction can be given by the number of molecules with

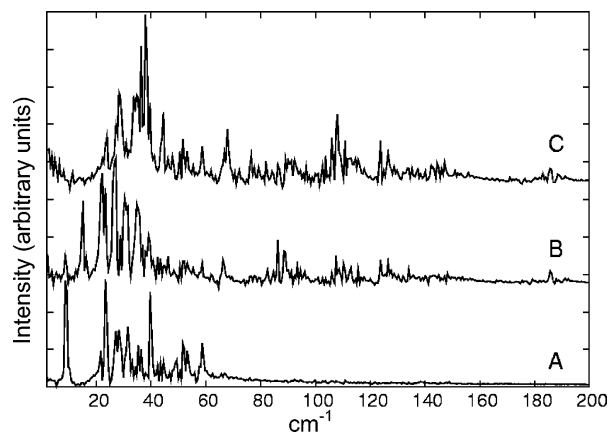


Figure 5. Fourier transform of the autocorrelation function of the transfer integrals between HOMOs of neighboring molecules (300 K). A vertical offset was introduced for clarity among the curves relative the transfer integral type A, B, and C.

the highest charge density that account for the 50% of the total (unit) excess charge, defined as $N_{50\%}$. The localization decreases as the energy of the eigenfunctions increases. The Boltzmann average of $N_{50\%}$ is 39, 36 and 31 molecules at 100, 200 and 300 K, respectively. At low temperature the disorder and the consequent localization is less pronounced but higher in energy and more delocalized states are less populated. The combination of these two factors causes a relatively modest effect of the temperature on the degree of localization of the wave function.

A convenient way to evaluate the role of the coupling dynamics is plotting the Fourier transform of the autocorrelation function $\langle \delta V_K(0) \delta V_K(t) \rangle$,¹⁰ shown in Figure 5 for the couplings A, B, and C (we have defined the deviation from the average transfer integral $\delta V_K(t) = V_K(t) - \langle V_K(t) \rangle$). The most important point is the majority of the phonon modes that modulate the coupling have energy around 40 cm^{-1} and the contribution of modes above 160 cm^{-1} is negligible. Because only low-frequency modes play a role in the modulation of the transfer integral, the semiclassical description adopted here can be considered valid at room temperature and at least plausible above 150 K (vibrations can be treated classically if their frequency ω is such that $\hbar\omega \ll k_B T$). The other important point is the dynamic disorder of organic crystals has a very long correlation time: $V_K(0)$ and $V_K(t)$ are correlated for a time longer than the MD simulation length (in such cases the correlation time is not precisely determinable). The long correlation distinguishes these systems from conductive liquid or liquid crystals.^{38,39} There is, as may be expected, some overlap between the peaks in Figure 4 and the Raman spectra of the pentacene,⁴⁰ a resemblance that we take as a confirmation of the reliability of the used force field. More in detail, there are 18 low-frequency optical modes in the pentacene crystal deriving from the combination of 6 intramolecular modes below 200 cm^{-1} and 3 hindered rotations (at energy of approximately 86, 114 and 140 cm^{-1})¹⁴ for each molecule in the unit cell. In agreement with the results of ref 14, essentially all these low-frequency modes modulate substantially at least one of the relevant intermolecular transfer integral because of their large amplitude.

Localization of electronic states in a solid is often associated with insulating states.^{35–37} However, the localization described here is dynamic and not due to static defects or self-trapped small polarons that lead to an activated transport regime. These localized states are mobile because they are very strongly coupled to other close localized states by the electron–phonon coupling term. One can see the charge carrier as being continuously scattered with very high probability at each

molecular site. For this reason dynamic localization is not in contrast with the high mobility observed recently for crystalline organic semiconductors such as rubrene⁴¹ or pentacene.^{20,21} We are currently working on the simulation of the electron dynamics in model systems characterized by a degree of disorder similar to that quantified in this paper.

The degree of localization and its characteristic time scales can be investigated by optical spectroscopy of field induced charge.⁴² The results obtained for different organic semiconductors^{43,44} indicate the presence of localized charge carrier also at low temperature (100 K), a picture that can be explained either by our model or by assuming the formation of a small polaron.

4. Discussion and Conclusion

The computational results presented here strongly point to an essential deficiency in the theoretical modeling of charge transport in organic material: *it is not possible to treat the electron–phonon coupling as a perturbation*. The modulation of the transfer integrals, due to low-frequency phonons, is of the same order of magnitude of their average values already above 100 K. The band description of the material breaks down because the k vector is not a good quantum number for these systems. Thermal disorder is able to localize the charge carrier within a few unit cells, preventing a description of the transport based on the carrier mean free path, which is consistent only with a delocalization of the carrier over a distance of many unit vectors. A similar behavior has been discussed for several metals, known as “bad metals”, and is related to the approaching of the electrons mean free path to the unit cell length.^{45,46} The thermal disorder discussed here for pentacene and anthracene is likely to be a general feature of many organic semiconductors, as indicated by previous⁴⁷ and underdevelopment studies on other organic compounds.

The huge overall modulation of the transfer integral V_{ij} is due to the high number of low-frequency modes that contribute independently to it (see Figure 5). In a typical perturbative approach, the effect of each phonon mode is treated independently through the electron–phonon coupling matrix elements taking the form of $\partial V_{ij} / \partial u_\lambda$ (u_λ is the nuclear displacement along the phonon mode λ).¹⁴ Although each coupling term can be relatively small, the global effect is dramatic if the unit cell contains tens of modes for which the coupling is not negligible (an essential difference between organic and inorganic semiconductors). The phonons in such systems affect the zeroth order description of the electronic wave function, making the theoretical modeling of the transport particularly challenging. The disorder of these materials is *dynamic* and a transport model should be able to describe the time evolution of localized states such as the ones depicted in Figure 5. The calculation presented in this paper suggests that a semiclassical numerical approach can be used to study the evolution of the charge carrier wave function in a model system characterized by few parameters characterizing its dynamical disorder, like the average amplitude of the modulation and the average frequency of the modulating phonons. Such a model is currently under investigation in our group.

It is useful to put the results of this paper in the framework of the general approach presented by Hannewald et al.,^{14,48} which starts from the following Hamiltonian:

$$H = \sum_{mn} V_{mn} a_m^\dagger a_n + \sum_{q\lambda} \hbar\omega_{q\lambda} \left(b_{q\lambda}^\dagger + b_{q\lambda} + \frac{1}{2} \right) + \sum_{q\lambda, mn} \hbar\omega_{q\lambda} g_{q\lambda, mn} (b_{q\lambda}^\dagger + b_{-q\lambda}^\dagger) a_m^\dagger a_n \quad (4)$$

where a_m^+ and a_m create and annihilate an electron at site m and $b_{q\lambda}^+$ and $b_{q\lambda}$ create and annihilate a phonon with wavevector \mathbf{q} in the mode λ (electrons and phonons are coupled by the last term of the Hamiltonian). The Hamiltonian of eq 4 is a starting point more general than ours (eq 1) because it is fully quantum mechanical and it includes the effect of local (Holstein) electron–phonon coupling. Its diagonalization is, however, a formidable task and several assumptions need to be introduced to describe the charge carrier wave function in specific transport regimes (with some loss of generality). Applying a canonical transformation akin to the “small polaron transformation”, the authors of ref 14 were able to transform eq 4 into

$$\tilde{H} = \sum_{mn} \tilde{V}_{mn} a_m^+ a_n + \sum_{q\lambda} \hbar\omega_{q\lambda} \left(b_{q\lambda}^+ b_{q\lambda} + \frac{1}{2} \right) \quad (5a)$$

$$\tilde{V}_{mn} = (e^C W e^{-C})_{mn} \quad W_{mn} = V_{mn} - \sum_{q\lambda, mn} \hbar\omega_{q\lambda} (g_{q\lambda} g_{-q\lambda})_{mn} \quad (5b)$$

with $C = \sum_{q\lambda, mn} g_{q\lambda, mn} (b_{q\lambda}^+ - b_{-q\lambda})$. Equation 5a looks like the Hamiltonian of noninteracting electron and phonons; however, the electron–phonon coupling is hidden in \tilde{V}_{mn} , which contains the phonon operator C . The authors assumed that the transport is bandlike, i.e., that the phase coherence is maintained and the phonon occupation number remains constant (i.e., the phonon assisted hopping is not important and scattering by phonon is infrequent). Under this assumption, valid at sufficiently low temperature, one can replace \tilde{V}_{mn} with its thermal average $\langle \tilde{V}_{mn} \rangle_T$ leading to an effective temperature-dependent polaronic band describing the state of the charge carrier dressed by phonons. With our paper we suggest that the last approximation ceases to be valid at temperatures above ~ 100 K, because the variance of the intermolecular coupling is large compared to its average value. Our approach, on the other hand, cannot be extended toward the low-temperature limit (because it is limited to classical phonons).⁴⁹ The two approaches can be seen as complementary because they are optimal in two different transport regimes.

It is, of course, very difficult to devise a model that is valid under different transport regimes, and further studies are necessary to define more precisely the temperature range under which bandlike transport and dynamic localization dominate. Moreover, in this paper we have neglected the coupling terms that contribute to the small polaron formation and that stabilize the charge on a single molecular site (Holstein coupling). If the transport is completely dominated by thermal hopping of small polarons, dynamic localization becomes less important. A more general approach, outside the scope of this paper, should consider at the same time the localization induced by the disorder in the transfer integral and the localization due to the Holstein coupling. Hopefully, further theoretical investigations will be stimulated by our computational finding.

We finally comment on the use of computational chemistry made in this paper. It is very common to adopt a transport model and to use computational methods as a simple bridge between the model and the experimental observables. However, if the model is wrong or inconsistent with the results of the computations themselves, the results are meaningless. In this paper computational chemistry methods contribute to the definition of a transport model, indicating that a pure band transport model cannot provide a consistent picture in the case of organic semiconductors at room temperature. We suggest that the effect of thermal disorder on the intermolecular transfer integrals can

be the missing ingredient in the description of the transport in organic semiconductors.

References and Notes

- (1) Dimitrakopoulos, C. D.; Malenfant, P. R. L. *Adv. Mater.* **2002**, *14*, 99.
- (2) Katz, H. E. *Chem. Mater.* **2004**, *16*, 4748.
- (3) Newman, C. R.; Frisbie, C. D.; da Silva, D. A.; Bredas, J. L.; Ewbank, P. C.; Mann, K. R. *Chem. Mater.* **2004**, *16*, 4436.
- (4) Karl, N. *Synth. Met.* **2003**, *133*, 649.
- (5) Jurchescu, O. D.; Baas, J.; Palstra, T. T. M. *Appl. Phys. Lett.* **2004**, *84*, 3061.
- (6) Cheng, Y. C.; Silbey, R. J.; da Silva Filho, D. A.; Calbert, J. P.; Cornil, J.; Bredas, J. L. *J. Chem. Phys.* **2003**, *118*, 3764.
- (7) Kenkre, V. M.; Andersen, J. D.; Dunlap, D. H.; Duke, C. B. *Phys. Rev. Lett.* **1989**, *62*, 1165.
- (8) de Wijs, G. A.; Mattheus, C. C.; de Groot, R. A.; Palstra, T. T. M. *Synth. Met.* **2003**, *139*, 109.
- (9) Jordan, K. D.; Paddon-Row, M. N. *Chem. Rev.* **1992**, *92*, 395.
- (10) Troisi, A.; Nitzan, A.; Ratner, M. A. *J. Chem. Phys.* **2003**, *119*, 5782.
- (11) Troisi, A.; Orlandi, G. *J. Phys. Chem. B* **2002**, *106*, 2093.
- (12) Balabin, I. A.; Onuchic, J. N. *Science* **2000**, *290*, 114.
- (13) Troisi, A.; Ratner, M. A.; Zimmt, M. B. *J. Am. Chem. Soc.* **2004**, *126*, 2215.
- (14) Hannewald, K.; Stojanovic, V. M.; Schellekens, J. M. T.; Bobbert, P. A.; Kresse, G.; Hafner, J. *Phys. Rev. B* **2004**, *69*, 075211.
- (15) Giuggioli, L.; Andersen, J. D.; Kenkre, V. M. *Phys. Rev. B* **2003**, *67*, 045110.
- (16) Stassen, A. F.; de Boer, R. W. I.; Iosad, N. N.; Morpurgo, A. F. *Appl. Phys. Lett.* **2004**, *85*, 3899.
- (17) Bussac, M. N.; Picon, J. D.; Zuppiroli, L. *Europhys. Lett.* **2004**, *66*, 392.
- (18) Coropceanu, V.; Malagoli, M.; da Silva Filho, D. A.; Gruhn, N. E.; Bill, T. G.; Bredas, J. L. *Phys. Rev. Lett.* **2002**, *89*, 275503.
- (19) Mahan, G. D. *Many-Particle Physics*, 3rd ed.; Plenum: New York, 2000.
- (20) Lin, Y.-Y.; Gundlach, D. J.; Nelson, S. F.; Jackson, T. N. *IEEE Trans. Elect. Dev.* **1997**, *44*, 1325.
- (21) Klauk, H.; Gundlach, D. J.; Nichols, J. A.; Jackson, T. N. *IEEE Trans. Elect. Dev.* **1999**, *46*, 1258.
- (22) Zhang, Y.; Petta, J. R.; Ambily, S.; Shen, Y.; Ralph, D. C.; Malliaras, G. G. *Adv. Mater.* **2003**, *15*, 1632.
- (23) Mattheus, C. C.; Dros, A. B.; Baas, J.; Oostergetel, G. T.; Meetsma, A.; de Boer, J. L.; Palstra, T. T. M. *Synth. Met.* **2003**, *138*, 475.
- (24) Torsi, L.; Dodabalapur, A.; Rothberg, L. J.; Fung, A. W. P.; Katz, H. E. *Science* **1996**, *272*, 1462.
- (25) Troisi, A.; Orlandi, G. *J. Phys. Chem. B* **2005**, *109*, 1849.
- (26) Mattheus, C. C.; Dros, A. B.; Baas, J.; Meetsma, A.; de Boer, J. L.; Palstra, T. T. M. *Acta Crystallogr. C* **2001**, *C57*, 939.
- (27) Allinger, N. L.; Li, F.; Yan, L.; Tai, J. C. *J. Comput. Chem.* **1990**, *11*, 868.
- (28) Berendsen, H. J. C.; Postma, J. P. M.; van Gunsteren, W. F.; di Nola, A.; Haak, J. R. *J. Chem. Phys.* **1984**, *81*, 3684.
- (29) Andersen, H. C. *J. Comput. Phys.* **1983**, *52*, 24.
- (30) Kundrot, C. E.; Ponder, J. W.; Richards, F. M. *J. Comput. Chem.* **1991**, *12*, 402.
- (31) Dudek, M. J.; Ponder, J. W. *J. Comput. Chem.* **1995**, *16*, 791.
- (32) Bredas, J. L.; Beljonne, D.; Coropceanu, V.; Cornil, J. *Chem. Rev.* **2004**, *104*, 4971.
- (33) Brock, C. P.; Dunitz, J. D. *Acta Crystallogr. B* **1990**, *46*, 795.
- (34) It is not possible to compare directly these data with the computation of the electron–phonon coupling in ref 14. However, in the high-temperature limit, the total contribution of the off-diagonal electron–phonon coupling terms in ref 14 is of the order of $k_B T$ in qualitative agreement with our computation (i.e., similar conclusion can be drawn for the role of thermal disorder).
- (35) Anderson, P. W. *Phys. Rev.* **1958**, *109*, 1492.
- (36) Lee, P. A.; Ramakrishnan, T. V. *Rev. Mod. Phys.* **1985**, *57*, 287.
- (37) Unge, M.; Stafstrom, S. *Synth. Met.* **2003**, *139*, 239.
- (38) Pecchia, A.; Lozman, O. R.; Movaghar, B.; Boden, N.; Bushby, R. J.; Donovan, K. J.; Kreouzis, T. *Phys. Rev. B* **2002**, *65*, 104204.
- (39) Palenberg, M. A.; Silbey, R. J.; Malagoli, M.; Bredas, J. L. *J. Chem. Phys.* **2000**, *112*, 1541.
- (40) Della Valle, R. G.; Venuti, E.; Farina, L.; Brillante, A.; Masino, M.; Girlando, A. *J. Phys. Chem. B* **2004**, *108*, 1822.
- (41) Stingelin-Stutzmann, N.; Smits, E.; Wondergem, H.; Tanase, C.; Blom, P.; Smith, P.; de Leeuw, D. *Nature Mater.* **2005**, *4*, 601.
- (42) Ziemelis, K. E.; Hussain, A. T.; Bradley, D. D. C.; Friend, R. H.; Ruhe, J.; Wegner, G. *Phys. Rev. Lett.* **1991**, *66*, 2231.
- (43) Brown, P. J.; Siringhaus, H.; Harrison, M.; Shkunov, M.; Friend, R. H. *Phys. Rev. B* **2001**, *63*, 125204.

- (44) Chang, J. F.; Sun, B. Q.; Breiby, D. W.; Nielsen, M. M.; Solling, T. I.; Giles, M.; McCulloch, I.; Sirringhaus, H. *Chem. Mater.* **2004**, *16*, 4772.
- (45) Gurvitch, M. *Phys. Rev. B* **1981**, *24*, 7404.
- (46) Ruzicka, B.; Degiorgi, L.; Berger, H.; Gaál, R.; Forró, L. *Phys. Rev. Lett.* **2001**, *86*, 4136.
- (47) Troisi, A.; Orlandi, G.; Anthony, J. A. *Chem. Mat.* **2005**, *17*, 5024.

- (48) Hannewald, K.; Bobbert, P. A. *Appl. Phys. Lett.* **2004**, *85*, 1535.

(49) We also note that, to compute the mobility from the Hamiltonian in eq 5, one also need some additional information about the scattering probability of a carrier in a state k of the polaronic band. In the dynamic localization regime, the $V(t)$ (eq 1) contains all the information required to compute the mobility; i.e., $V(t)$ can be used to determine the diffusion of the localized carrier.